JOURNAL OF SOLID STATE CHEMISTRY 63, 401–408 (1986)

Magnetic Properties of $TlFe_{2-x}Se_2$

L. HÄGGSTRÖM, H. R. VERMA,* S. BJARMAN, AND R. WÄPPLING

Institute of Physics, Uppsala University, Box 530, 751 21 Uppsala, Sweden

AND R. BERGER†

Materials Science Centre of the University, Laboratory of Inorganic Chemistry, Nijenborgh 16, 9749 AG Groningen, The Netherlands

Received October 3, 1985

Mössbauer studies on a mosaic of single crystals of the layered compound $TlFe_{2-x}Se_2$ have been carried out at various temperatures between 100 and 460 K. A magnetic transition occurs at ~450 K. The magnetic ordering within the Fe–Se layers is antiferromagnetic with the spins oriented along the tetragonal axis. X-Ray diffraction data indicated ordering of the iron vacancies at the chosen composition ($x \sim 0.3$) yielding a supercell with a volume five times that of the $ThCr_2Si_2$ type subcell, the cell parameters being $a = 8.6909(5)$ Å and $c = 14.005(1)$ Å.

Introduction

The compound $TlFe_2Se_2$ was claimed to crystallize in the $ThCr_2Si_2$ type structure (*1*). The iron atoms form a two-dimensional simple square lattice, each iron at the center of slightly irregular tetrahedra of selenium atoms which are interconnected to a network. These Fe–Se layers are separated by thallium atoms making interlayer selenium bonds impossible. The structure is given in Fig. 1. The magnetic properties of this layer compound have not been investigated before. In the present paper information on the magnetic structure and the magnetic transition, as obtained by Mössbauer spectroscopy, is reported.

* On leave from Physics Department, Punjabi University, Patiala, India.

† Present address: Institute of Chemistry, Uppsala University, Box 531, 751 21 Uppsala, Sweden.

Experimental

The sample was made from mixing Tl_2Se, Fe, and Se and reacting the materials in a silica-tube synthesis first at 670 K. After homogenization by grinding, the product was further heat-treated at 970 K for 3 days and subsequently quenched. The final product consisted mainly of aggregates of flaky crystals. After removing a small amount of unreacted iron powder, X-ray powder patterns were recorded by means of a Guinier-Hägg camera with strictly monochromatic $CuK\alpha_1$ radiation ($\lambda = 1.540596$ Å) using silicon as internal calibration standard ($a = 5.431065$ Å).

Mössbauer spectra of a mosaic of small single crystals—oriented on a thin aluminum backing so that the *c*-axis was parallel to the γ-ray direction—were recorded using a conventional constant acceleration spectrometer. The thickness of the crystal

0022-4596/86 $3.00

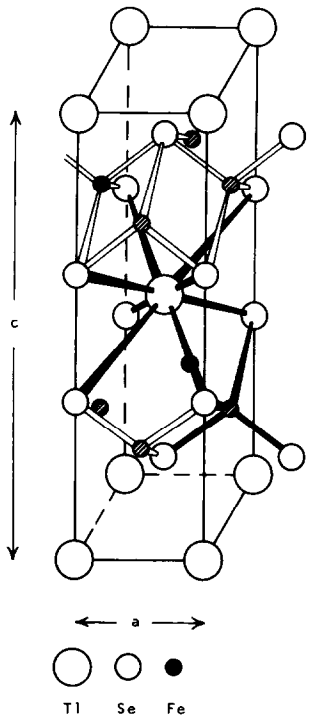

FIG. 1. The crystal structure of stoichiometric $TlFe_2Se_2$.

flakes was typically 35 μm. A $^{57}Co(Rh)$ source kept at room temperature was used, the spectra being recorded in the range 100 to 460 K. Calibration spectra were taken simultaneously on the double-ended electrochemical drive. The analysis was made by means of a least-squares fitting program (*2*).

Results and Discussion

The X-ray powder patterns could be indexed on a body-centered tetragonal cell yielding cell parameters in good agreement with the data given for $TlFe_2Se_2$ given by Klepp and Boller (*1*). However, additional hardly detectable lines on the diffraction photograph showed that the sample was insufficiently characterized. In order to improve the line quality, powdered material, kept in an evacuated capillary, was shortly heat-treated in a flame. This treatment made all lines sharper, including the weak ones which now became quite measurable. It was found that by choosing an a-axis $\sqrt{5}$ times greater than that suggested by Klepp and Boller all lines of the pattern could be indexed. Obviously, the new body-centered tetragonal cell is a supercell based on the $ThCr_2Si_2$ type structure. The film data are presented in Table I. The appearance of the larger unit cell is probably an effect of ordering of vacancies. Since we noticed unreacted iron, the synthesis product is likely to be iron deficient corresponding to the formula $TlFe_{2-x}Se_2$ where $0 < x < 1$.

Electron microprobe analyses were performed to confirm this hypothesis. The result after correction for absorption and fluorescence was $x = 0.28(7)$. Similar nonstoichiometry in the Tl–Fe–S system was found by Sabrowsky *et al.* (*3*) who indicated the same kind of supercell for $TlFe_{1.6}S_2$ as found from neutron diffraction data. Contrary to Klepp and Boller (*1*), nonstoichiometry of $TlFe_2Se_2$ was suggested by Sabrowsky *et al.* (*4*). Neither the homogeneity range nor the cell parameters were reported. We made syntheses of deliberately nonstoichiometric $TlFe_{2-x}Se_2$ with $x = 0.4$ and 0.6 which suggest a linear relationship between the subcell axes (no supercell reflexions detected for $x = 0.6$) and the iron composition. The iron-rich limit of the homogeneity range corresponds to $x \sim 0.3$ at 970 K.

Above 450 K, the Mössbauer spectrum of $TlFe_{2-x}Se_2$ shows only an asymmetric doublet. Below 450 K, a magnetic pattern is also observed, the intensity of which increases at the expense of that of the doublet on lowering the temperature. Representative spectra are given in Fig. 2. At 295 K, only the magnetic pattern remains, apart from a low intensity (~7%) single line at 0.38 mm/s, probably originating from iron in the aluminum backing foil (*5*).

TABLE I

X-RAY POWDER DIFFRACTION DATA OF TETRAGONAL $TlFe_{1.7}Se_2$

Intensity (obs.)	$Q \times 10^5$ (Å^{-2}) obs.	calc.	$h\ k\ l$	Intensity (obs.)	$Q \times 10^5$ (Å^{-2}) obs.	calc.	$h\ k\ l$
vw	1866	1834	1 0 1*	vw	42115	42186	3 3 6*
w-	2041	2039	0 0 2	vw	43052	42983	5 2 3*
w-	2639	2648	1 1 0*	w	44834	44834	4 2 6
w-	4677	4687	1 1 2*	vw	45012	45014	5 3 0*
w-	5284	5296	2 0 0*	m-	45842	45845	5 0 5
vw	5943	5913	1 0 3*				4 3 5
m	7128	7130	2 1 1			45870	3 1 8
vw	7316	7335	2 0 2*	w	47910	47918	2 1 9
w	8158	8158	0 0 4	m-	53016	52958	6 2 0
vst	11196	11208	2 1 3	vw	58077	58081	5 0 7
w-	12628	12631	2 2 2*				4 3 7
st	13229	13239	3 1 0	m-	59110	59109	4 2 8
vw	13488	13453	2 0 4*	vw	60117	60087	6 3 1
vw	14041	14070	1 0 5*	vw	61128	61115	6 2 4
st	15265	15279	3 1 2	m-	64214	64166	6 3 3
w	18355	18355	0 0 6			64225	3 1 10
vw	18718	18749	2 2 4*	w	66234	66197	5 5 0
m	19358	19366	2 1 5				7 1 0
vw	21176	21183	4 0 0*	m-	68338	68236	5 5 2
w-	21400	21397	3 1 4				7 1 2
st	26490	26479	4 2 0			68312	2 1 11
vw	28487	28518	4 2 2	w-	71369	71312	6 2 6
st	31599	31594	3 1 6	w-	72361	72324	6 3 5
w	32631	32631	0 0 8	vw	73506	73419	0 0 12
w	33635	33608	5 0 1	w	74435	74397	5 0 9
			4 3 1				4 3 9
w	34616	34637	4 2 4	w	84533	84552	5 5 6
vw	36374	36462	5 1 2*				7 1 6
st	37685	37687	5 0 3	vw	85529	85588	6 2 8
			4 3 3				

Note. The reflexions are represented by their Q-values ($= d^{-2}$). The indices apply to the refined cell, a = 8.6909(5) Å and c = 14.0048(11) Å, the figures within parenthesis denoting the estimated standard deviations as obtained from the weighted least-squares refinement. Those reflexions which cannot be indexed on the $ThCr_2Si_2$ type subcell are indicated by an asterisk.

A closer inspection of the spectrum at 295 K reveals that the outer lines (lines 1 and 6 of an ordinary six-line magnetic pattern) are of unequal intensity. The inner lines (lines 3 and 4) are, on the contrary, of almost equal intensity. Line 5 is absent while line 2 seems to occur at ~−1.5 mm/s. However, an analysis discloses that line 2, if it were present, should appear at a more negative velocity. The line at −1.5 mm/s can be interpreted as the first line of an *additional* six-line pattern, line 6 of which coincides with line 6 of the main phase. This explains the mentioned difference in intensity of the outer lines.

The parameters obtained from the least-squares fits are given in Table II. The additional component (intensity ~8%), corre-

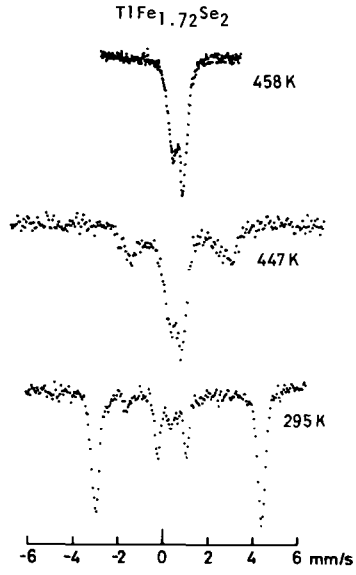

FIG. 2. Mössbauer spectra of $TlFe_{1.7}Se_2$ at different temperatures.

sponding to a magnetic field and an isomer shift versus natural iron at 295 K of 18.1(2) T and 0.88(3) mm/s, respectively, shows a similar temperature variation of the magnetic hyperfine field as the main component of the Mössbauer spectrum.

The occurrence of a supercell with a cell volume five times that of the basic structure indicates 1/5 vacancies which would yield the composition $TlFe_{1.60}Se_2$. In the simplest model, independently conceived by Sabrowsky *et al.* for a corresponding sulfide (*3*), all iron atoms take three iron neighbors in the square lattice (Fig. 3). However, the electron microprobe analysis gave for the present sample the composition $TlFe_{1.72(7)}Se_2$. Hence, some iron (~7(4)%) may partly occupy the otherwise vacant sites. Preliminary calculations of the X-ray diffraction intensities of the corresponding powder pattern support this structure model. The additional component of the Mössbauer spectra ($T < 450$ K) may therefore arise from these iron atoms having another coordination than the rest. The temperature covariation of the hyperfine fields suggests this interpretation. On the other hand, the difference in isomer shift values (~0.3 mm/s) between iron atoms having three or four other iron atoms as near neighbors seems too large.

Another explanation would be the presence of another phase. There is contradictory information as regards the ternary phases of the Tl–Fe–Se system, and virtually nothing is known about thermal stability and homogeneity ranges. We cannot exclude that the iron content of the tetragonal phase is lowered on decreasing the temperature. It may even be so that a two-phase mixture of iron and monoclinic $TlFeSe_2$ (*6*) represents the equilibrium situation. An additional crystalline ternary phase would probably be detected by powder diffraction if its content is more than 2 wt%. However, an iron selenide (taking part in a three-phase equilibrium?) would scatter very little compared with a thallium-containing matrix, but may compete as regards the Mössbauer signals.

The fact that lines 2 and 5 are absent in the $TlFe_{2-x}Se_2$ spectra shows that the iron spins are parallel with the γ-ray direction,

TABLE II

^{57}Fe MÖSSBAUER PARAMETERS FOR $TlFe_{1.7}Se_2$

T (K)	B (T)	δ (mm/s)	ΔE_Q (mm/s)	W_1 (mm/s)
100	27.2(1)	0.68(1)	0.26(3)	0.40(2)
295	23.0(1)	0.55(1)	0.28(3)	0.29(2)
423	16.7(2)	0.47(1)	0.2 (1)	0.35(2)
433	15.4(2)	0.45(1)	0.2 (1)	0.40(3)
438	14.7(2)	0.46(1)	0.2 (1)	0.39(5)
441	14.2(2)	0.45(1)	0.2 (1)	0.40(5)
444	14.0(2)	0.46(1)	0.2 (1)	0.45(5)
447	13.7(2)	0.45(1)	0.2 (1)	0.47(5)
458	—	0.44(1)	0.48(1)	0.33(2)

Note. B is the magnetic hyperfine field, δ the isomer shift relative to iron metal at room temperature, ΔE_Q the electric quadrupole splitting as defined in the text, and W is the FWHM linewidth.

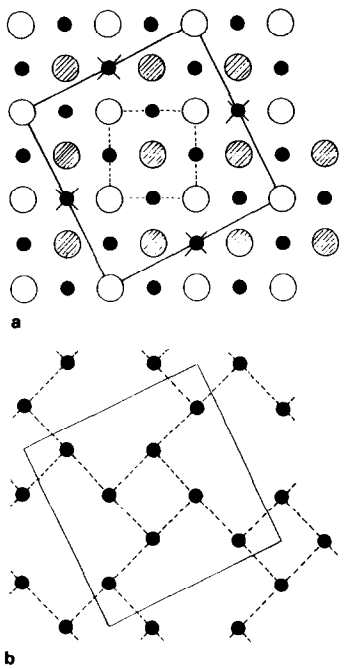

FIG. 3. (a) Tentative structure (I 4/m) of $TlFe_{2-x}Se_2$ (based on the $ThCr_2Si_2$ type with ordered vacancies) projected on (001). (●) Fe site, $z = \frac{1}{4}$ and $\frac{3}{4}$; (○) Tl site, $z = 0$; (⊘) Tl site, $z = \frac{1}{2}$; (✖) site totally vacant ($TlFe_{1.6}Se_2$) or partly occupied by Fe, $z = \frac{1}{4}$ and $\frac{3}{4}$. The Se sites, situated $\Delta z = 0.36$ relative to the Tl sites, were omitted for clarity. The solid lines give the unit cell of the ordered structure while the subcell is indicated by the dotted lines. (b) An iron atom layer (cf. (a)) of $TlFe_{1.6}Se_2$ drawn relative the supercell showing that each iron atom has got three near iron neighbors. Partial filling of the vacancy yields a change in coordination number to four, occurring for $TlFe_{2-x}Se_2$, $0 < x < 0.4$.

i.e., with the tetragonal c-axis of the single crystals. In the absence of an external magnetic field it is not possible to distinguish between a ferromagnet and an antiferromagnet from the Mössbauer spectrum. The crystals are, however, not attracted by a magnet from which we conclude that $TlFe_{2-x}Se_2$ is an antiferromagnet.

Using the structural parameters of the subcell given by Klepp and Boller (*1*), the closest interatomic distances for iron are Fe–Se (×4) 2.46 Å and Fe–Fe (×4) 2.75 Å. The distances involving thallium are Tl–Se (×8) 3.40 Å and Tl–Fe (×8) 4.00 Å. The latter figure implies a relatively large separation between iron atoms of different Fe–Se layers. We therefore expect a weaker interaction between the layers than within them.

The isomer shift value for the iron atoms of the main spectrum and the strength of the electric quadrupole interaction (Table II) are consistent with iron either in a high-spin Fe^{3+}, a metallic, or in a highly covalent state (*7*). The magnitude of the magnetic hyperfine field excludes the first alternative. Selenium is known to form strongly covalent bonds and, since the iron atoms are bound only to selenium, a large covalency is not unexpected.

The magnetic interaction between the iron atoms may proceed in two ways, either through conduction electron polarization or through the covalent selenium bonds. The shortest Fe–Fe distance of 2.75 Å may allow for spin polarization via the conduction electrons. The sign of the exchange integral varies with distance in a critical manner; both ferro- and antiferromagnetic coupling is possible. On the other hand, a large covalency is usually accompanied by strong superexchange interactions leading to antiferromagnetic coupling between the magnetic moments.

The bond angles Fe–Se–Fe in $TlFe_{2-x}Se_2$ are ~67° and ~103°, respectively, which might not seem favorable for superexchange. However, there are two amplifying effects: at 90° one expects the interaction between atoms having a d^5 configuration to be particularly strong and the same tendency occurs for selenium ligands (*8*). Even in the d^6 case, which is less favorable for superexchange, one finds antiferromagnetic ordering in selenium compounds as exemplified by $FeRh_2Se_4$ (*9*). In that compound, iron has only selenium neighbors at a similar distance (2.5 Å) as in $TlFe_{2-x}Se_2$ and the bond angle is 93°.

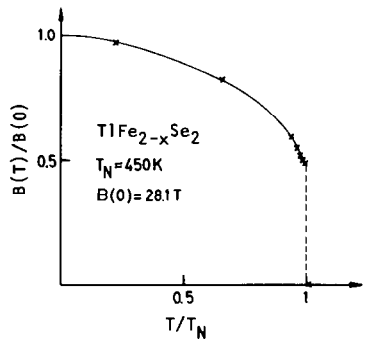

FIG. 4. Temperature variation of the reduced magnetic field (main component).

Due to the large distance between the Fe–Se layers (7 Å) we propose that the antiferromagntic ordering occurs within the layers in $TlFe_{2-x}Se_2$, with the spins oriented along the tetragonal axis. For comparison, Sabrowsky *et al.* (*3*) reported a similar Mössbauer spectrum of $TlFe_{1.6}S_2$ and concluded from neutron diffraction data that no three-dimensional order occurs down to 16 K. A similar situation may very well obtain for the selenide, the interaction being weak between the layers.

Figure 4 shows the variation of the hyperfine field with temperature, while Fig. 5 shows the variation of the relative intensity of the magnetic component. As can be seen, the compound successively transforms from the magnetic to the nonmagnetic state long before the hyperfine field value has dropped to zero. The transition at ~450 K is evidently of first order as revealed by the sudden drop of the magnetic field and by the presence of a temperature hysteresis of the magnetic/nonmagnetic intensity ratio. At 433 K, the ratio is, respectively, 1.2(1) or 1.4(1) on increasing or decreasing the temperature. The appearance of a two-phase region around T_N can be explained as due to nucleation processes in the single crystals (*10*). We expect that the first-order transition is accompanied by changes in the lattice distances as in $FePS_3$ (*11*), which also has a layered structure, or in the positional parameters within the cell. We have not been able to investigate this. The transition at T_N involves a heat effect as revealed by differential thermal analysis; an endothermic peak was obtained on heating.

The electric quadrupole splitting above T_N can be written as

$$\Delta E_Q^p = \left| \frac{eQV_{zz}}{2} \sqrt{1 + \frac{\eta^2}{3}} \right|$$

where V_{zz} and η are the principal component and the asymmetry parameter of the electric field gradient (EFG) tensor, respectively. Q is the quadrupole moment of the iron nucleus in its excited state. Below T_N, ΔE_Q is in first-order perturbation theory defined by (*12*)

$$\Delta E_Q^m = \frac{3\cos^2\theta - 1 + \eta \sin^2\theta \cos 2\phi}{2} \cdot \frac{eQV_{zz}}{2}.$$

Here, θ and ϕ stand for the polar and azimuthal angles of the magnetic field vector in the principal system of the EFG tensor.

Normally, the factor eQV_{zz} does not vary over the transition temperature, and a ratio R can be defined as

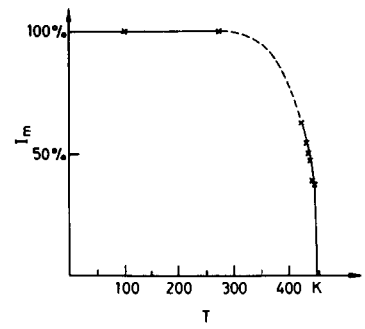

FIG. 5. Relative intensity of the magnetic main component as a function of temperature.

$$R = \frac{\Delta E_Q^m}{\Delta E_Q^p} = \frac{3\cos^2\theta - 1 + \eta\sin^2\theta\cos 2\phi}{\pm 2\sqrt{1 + \frac{\eta^2}{3}}}.$$

In the present case, $R = +0.27(3)/\pm 0.48(1) = \pm 0.56(7)$. The symmetry around the iron atoms is such that one of the principal axes of the EFG tensor coincides with the crystallographic c-axis. The polar angle θ can then either take the value 0° or 90°. For $\theta = 0°$, R is close to unity, while for $\theta = 90°$, $-0.87 < R < 0$. The magnitude of R thus favors $\theta = 90°$ and the negative sign for R. Furthermore, the value of η is less than 0.2 whence the most probable value for ϕ is 90°. The orientation of the principal system of the EFG tensor is thus established with V_{zz} and V_{xx} in the c-plane and V_{yy} along the tetragonal axis giving the electric quadrupole strength $eQV_{zz}/2 = -0.48(2)$ mm/s.

The consistency of this choice of sign can be obtained from the asymmetry found in the doublet above T_N. For $V_{zz} < 0$, the intensity ratio between the two lines is given by (*13*)

$$I_R = \frac{I(\text{high-velocity peak})}{I(\text{low-velocity peak})} = \frac{4\sqrt{1 + \eta^2/3} - (3\cos^2\alpha - 1 + \eta\sin^2\alpha\cos 2\beta)}{4\sqrt{1 + \eta^2/3} + (3\cos^2\alpha - 1 + \eta\sin^2\alpha\cos 2\beta)}.$$

Here, α and β are the polar and azimuthal angles of the γ-ray direction in the EFG principal axis system. Since in this special case the γ-ray direction is parallel with the magnetic hyperfine field, $\alpha = \theta$ and $\beta = \phi$, we only need to use the latter symbols. By putting

$$\frac{3\cos^2\theta - 1 + \eta\sin^2\theta\cos 2\phi}{2} = K$$

and

$$\sqrt{1 + \eta^2/3} = A$$

the expression for R and I_R can be written as

$$R = \frac{K}{A} \text{ and } I_R = \frac{2A - K}{2A + K}$$

leading to

$$I_R = \frac{2 - R}{2 + R}.$$

With $R = -0.56(7)$ we obtain $I_R = 1.78(13)$ to be compared with the experimental value of $I_R = 1.5(1)$. The latter value has not been corrected for saturation effects due to the finite absorber thickness. A correction would increase the experimental value of I_R. We therefore conclude that the two values of I_R are not significantly different.

The quadrupole splitting and isomer shift at room temperature of $TlCuFeSe_2$ have been determined as, respectively, $|0.81(1)|$ and 0.57(1) mm/s (*14*). It is isostructural with the ideal stoichiometric $TlFe_2Se_2$, i.e., of the $ThCr_2Si_2$ type. While the values of the isomer shift are very similar, the quadrupole splitting of $TlCuFeSe_2$ is markedly different from the value of $-0.48(1)$ mm/s. Systematic work on the system $TlCu_{2-x}Fe_xSe_2$ is needed to explain this difference.

Acknowledgments

R.B. gives thanks for the monetary support from The Netherlands Foundation for Chemical Research and The Netherlands Organization for the Advancement of Pure Research. The stay at the laboratories of Rijksuniversiteit Groningen was personally promoted by Professor F. Jellinek and Dr. C. F. van Bruggen which is gratefully acknowledged.

References

1. K. KLEPP AND H. BOLLER, *Monatsh. Chem.* **109**, 1049 (1978).

2. P. JERNBERG AND T. SUNDQVIST, Uppsala University, Institute of Physics, Report UUIP-1091 (1983).
3. H. SABROWSKY, D. WELZ, P. DEPPE, M. ROSENBERG, AND W. SCHÄFER, VIII Internat. Conf. on Solid Compounds of Transition Elements, Vienna (1985).
4. H. SABROWSKY, J. MIRZA, AND C. METHFESSEL, *Z. Naturforsch. B: Anorg. Chem. Org. Chem.* **34,** 115 (1979).
5. R. S. PRESTON AND R. GERLACH, *Phys. Rev. B: Condens. Matter* **3,** 1519 (1971).
6. K. KLEPP AND H. BOLLER, *Monatsh. Chem.* **110,** 1045 (1979).
7. R. INGALLS, F. VAN DER WOUDE, AND G. A. SAWATZKY, *in* "Mössbauer Isomer Shifts" (G. K. Shenoy and F. E. Wagner, Eds.), North-Holland, Amsterdam (1978).
8. P. W. ANDERSON, *in* "Magnetism I" (G. T. Rado and S. Suhl, Eds.), Academic Press, New York (1963).
9. H. N. OK, K. S. BAEK, AND C. S. KIM, *Phys. Rev. B: Condens. Matter* **26,** 4436 (1982).
10. C. B. BEAN AND D. S. RODBELL, *Phys. Rev.* **126,** 104 (1962).
11. S. BJARMAN, P. JERNBERG, AND R. WÄPPLING, *Hyperfine Interact.* **15–16,** 625 (1983).
12. L. HÄGGSTRÖM, University of Uppsala, Institute of Physics, Report UUIP-851 (1971).
13. P. ZORY, *Phys. Rev. A* **140,** 1401 (1965).
14. R. BERGER AND C. F. VAN BRUGGEN, *J. Less-Common Met.* **113,** 291 (1985).